Proc. Natl. Acad. Sci. USA
Vol. 95, pp. 15014–15019, December 1998
Neurobiology

Phosphorylation of photolyzed rhodopsin is calcium-insensitive in retina permeabilized by α-toxin

(rhodopsin kinase/phototransduction/photoreceptor cells/cGMP)

ANNIE E. OTTO-BRUC†, ROBERT N. FARISS†, J. PRESTON VAN HOOSER†, AND KRZYSZTOF PALCZEWSKI†‡§¶

Departments of †Ophthalmology, ‡Pharmacology, and §Chemistry, University of Washington, Seattle, WA 98195-6485

Edited by Jeremy Nathans, Johns Hopkins University School of Medicine, Baltimore, MD, and approved October 20, 1998 (received for review September 10, 1998)

ABSTRACT **Light triggers the phototransduction cascade by activating the visual pigment rhodopsin (Rho → Rho*). Phosphorylation of Rho* by rhodopsin kinase (RK) is necessary for the fast recovery of sensitivity after intense illumination. Ca^{2+} ions, acting through Ca^{2+}-binding proteins, have been implicated in the desensitization of phototransduction. One such protein, recoverin, has been proposed to regulate RK activity contributing to adaptation to background illumination in retinal photoreceptor cells. In this report, we describe an *in vitro* assay system using isolated retinas that is well suited for a variety of biochemical assays, including assessing Ca^{2+} effects on Rho* phosphorylation. Pieces of bovine retina with intact rod outer segments were treated with pore-forming staphylococcal α-toxin, including an α-toxin mutant that forms pores whose permeability is modulated by Zn^{2+}. The pores formed through the plasma membranes of rod cells permit the diffusion of small molecules <2 kDa but prevent the loss of proteins, including recoverin (25 kDa). The selective permeability of these pores was confirmed by using the small intracellular tracer *N*-(2-aminoethyl) biotinamide hydrochloride. Application of [γ-^{32}P]ATP to α-toxin-treated, isolated retina allowed us to monitor and quantify phosphorylation of Rho*. Under various experimental conditions, including low and high $[Ca^{2+}]_{free}$, the same level of Rho* phosphorylation was measured. No differences were observed between low and high $[Ca^{2+}]_{free}$ conditions, even when rods were loaded with ATP and the pores were closed by Zn^{2+}. These results suggest that under physiological conditions, Rho* phosphorylation is insensitive to regulation by Ca^{2+} and Ca^{2+}-binding proteins, including recoverin.**

Among the signal transduction systems that have been studied, phototransduction in the vertebrate retina has emerged as one of the best understood. This process is initiated by photoactivation of rhodopsin (Rho) and proceeds through a series of highly specific protein interactions, culminating in closure of cation channels in the rod plasma membrane. To preserve the sensitivity of this signaling system, molecular mechanisms are required to return the photoactivated receptor (Rho*) to an inactive state. Receptor desensitization is accomplished through a multistep process beginning with the phosphorylation of the C terminus of Rho* by rhodopsin kinase (RK). Because of its crucial role in Rho* inactivation (reviewed in ref. 1), RK has been extensively studied, and a great deal is now known regarding RK's expression (2), its interactions with Rho* (3), and its role in human vision (4, 5).

Previous studies have reported that Rho* phosphorylation could be regulated by Ca^{2+} (6–9). Because RK does not have any recognizable Ca^{2+}-binding motifs, this effect is believed to be modulated by a Ca^{2+}-binding protein. *In vitro*, recoverin, in its Ca^{2+}-bound state, forms a complex with RK, thereby inhibiting RK activity. The interaction between RK and recoverin was significantly weakened by autophosphorylation of RK (10) or by inactivation of one of two functional Ca^{2+}-binding loops of recoverin (11). The inhibition of RK by recoverin was proposed to be one of the mechanisms of light adaptation (6, 12).

Conventional biochemical procedures, although invaluable for the study of complex physiological processes like phototransduction, have some significant drawbacks. Among these are necessary immense dilutions, omission of key components, and destruction of complex biological structures. Together, these factors confound attempts to recreate and analyze physiologically relevant processes. This has been illustrated in our studies of the sites of Rho* phosphorylation in which different results were obtained *in vitro* and *in vivo* (2, 13). Staphylococcal α-toxin, streptolysin-O, and *Escherichia coli* hemolysin are pore-forming bacterial toxins frequently employed in cell biology experiments that require diffusion of small molecules from the extracellular space into the cell. These single-chain polypeptides are water-soluble. On contact with cell membranes, toxin monomers assemble to form pores of uniform diameter that allow free passage of molecules through the plasma membranes (reviewed in refs. 14 and 15). Application of these pore-forming toxins is an alternative to electroporation (16) with advantages of controllable pore density and diameter. For our purposes, staphylococcal α-toxin (33.4 kDa) appears to be ideal for the permeabilization of rod outer segments (ROS). α-Toxin (also known as staphylococcal α-hemolysin) forms a heptameric pore with a diameter of 14 Å (17), allowing the passage of molecules smaller than 2 kDa (such as metal ions and nucleotides), yet retaining all proteins inside the cell. Walker *et al.* (18) have engineered a metal-activated version of this toxin. The pores were designed to be blocked and unblocked by the addition and removal of micromolar concentrations of Zn^{2+} (Fig. 1). A major technical problem in membrane permeabilization of ROS (e.g., by electroporation) is the poor quality of ROS preparations from sources other than amphibians. To study phototransduction in mammalian rods, we chose bovine retina, which has been the subject of numerous biochemical studies. Instead of employing partially purified and broken ROS, we treated trephine punches from whole retina with α-toxin and subjected them to light-dependent phosphorylation. Nucleotides are exchanged with extracellular medium through the pore, and selected extracellular buffers maintain intracellular

The publication costs of this article were defrayed in part by page charge payment. This article must therefore be hereby marked "*advertisement*" in accordance with 18 U.S.C. §1734 solely to indicate this fact.

This paper was submitted directly (Track II) to the *Proceedings* office.
Abbreviations: ICC, immunocytochemistry; OS, outer segments; RK, rhodopsin kinase; Rho, rhodopsin; Rho*, photoactivated Rho; ROS, rod outer segment(s).
¶To whom reprint requests should be addressed at: University of Washington, Department of Ophthalmology, Box 356485, Seattle, WA 98195-6485. e-mail: palczews@u.washington.edu.

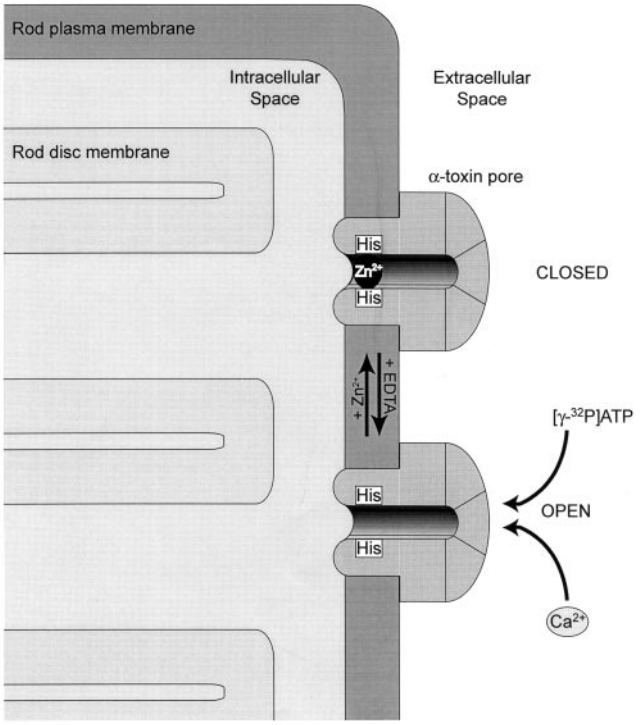

FIG. 1. Formation of a switchable pore in the plasma membrane of rod photoreceptors. α-Toxin of *Staphylococcus aureus* is a self-assembling, pore-forming protein. Heptameric α-toxin pores are inserted in the plasma membrane of rod cells, allowing nucleotide and ion exchange between intra- and extracellular compartments. In a mutated form of the toxin (H5K8A), the amino acids 130–134 have been replaced by five histidines to facilitate pore closure by Zn^{2+} ions. This mechanism is reversible by chelation of Zn^{2+} with EDTA. Note that the depicted components are not to scale.

$[Ca^{2+}]_{free}$ within a physiological range. The advantage of this assay system is that it retains the functional integrity of the retina *in vivo* and is amenable to biochemical studies. By employing this assay, we were able to ask whether $[Ca^{2+}]$ affects the rate of Rho* phosphorylation. In this study, we have found that Rho* phosphorylation is not under Ca^{2+} regulation, and we suggest that the function of recoverin is still subject to debate. The experimental approach developed in this study also may have general applications for the investigation of other phototransduction steps.

MATERIALS AND METHODS

Expression and Purification of α-Toxin. *E. coli* JM109 (DE3) transformed with pT7-NPH8S(K8A) (19) were grown in two liters of Luria–Bertani (LB) medium containing 100 μg/ml ampicillin (LB/amp) at 30°C overnight to an OD_{570} of 1.3–1.4. The bacterial pellet was resuspended in 50 mM Tris (pH 8.0) containing 150 mM NaCl and 50 mM EDTA, sonicated, and centrifuged at 125,000 × *g* for 60 min. Further purification was done by using ammonium sulfate precipitation followed by chromatography on SP-Sepharose FF (Amersham) according to the procedure described by Walker *et al.* (20). Typically, 5–6 mg of α-toxin was obtained. The K8A mutation in α-toxin did not affect pore formation but increased the expression levels of the toxin in *E. coli.* For the H5K8A mutated toxin, in which amino acids 130–134 were replaced by 5 histidine residues, the bacterial pellet was resuspended in 50 mM Tris (pH 8.0) containing 150 mM NaCl and 10 mM imidazole, sonicated, and centrifuged at 125,000 × *g* for 60 min. Purification was accomplished on Ni^{2+}-NTA agarose (Qiagen, Chatsworth, CA) according to Walker *et al.* (18).

Assay for Rho* Phosphorylation. Bovine eyes were obtained from a local slaughterhouse (Schenk Packing, Stanwood, WA). Trephine punches (7.5 mm in diameter) from fresh retina were kept in 0.5 ml of isoosmotic buffer [10 mM Hepes (pH 7.5)/120 mM NaCl/3.5 mM KCl/10 mM glucose/0.2 mM $CaCl_2$/0.2 mM $MgCl_2$/1 mM EDTA] containing 1 mM GTP and 1 mM NADPH. Typically, 50–100 μg/ml of α-toxin was added to the isoosmotic buffer. Three retina punches (per condition) were incubated for 30 to 45 min at room temperature to allow pore formation (in control experiments, the α-toxin was omitted), 1 mM [γ-^{32}P]ATP (40,000 cpm/nmol) was added, and after 3–5 min, the punches were exposed to light from a 433D flash lamp (Sun Pak, Tocad America, Hackensack, NJ), which bleached ≈10% of total Rho. After 5 min, the reaction was stopped by freezing the punches in dry ice/ethanol. For analysis, the samples were homogenized in sucrose-phosphate buffer [67 mM potassium phosphate (pH 7.0)/1 mM magnesium acetate/1 mM DTT/1 mM adenosine/4.1 mM EDTA/15 mM KF/10 mM ATP/35% sucrose (density 1.11)] and shaken for 30 min. ROS were purified on a continuous sucrose gradient (density 1.11 to 1.15). Gradients were centrifuged at 26,500 × *g* for 150 min. ROS then were collected and centrifuged at 86,000 × *g* for 15 min. Pellets were analyzed by using SDS/PAGE and autoradiography (X-Omat blue film, Kodak). Alternatively, punches were solubilized with 3 mM dodecyl β-D-maltoside in 10 mM Hepes (pH 7.5) containing phosphatase and kinase inhibitors (1 mM adenosine/4.0 mM EDTA/15 mM KF/10 mM ATP). After centrifugation, the supernatant was mixed with an anti-Rho mAb(C7)-Sepharose. mAb(C7)-Sepharose was then washed with 10 mM Hepes (pH 7.5) containing 0.4 mM dodecyl β-D-maltoside and the phosphatase and kinase inhibitors. Bound proteins were eluted with 0.1 M glycine (pH 2.5) and 0.4 mM dodecyl-β-D-maltoside. Eluted proteins were analyzed by using SDS/PAGE and autoradiography. In most experiments, the amount of Rho loaded on SDS/PAGE gels was 200 pmol. The intensity of radiolabeling was ≈5 pmol of phosphate, and the bleaching was ≈10% of Rho, as measured by changes in absorption at 498 nm. For phosphorylation time courses, autoradiograms and SDS/PAGE gels were scanned, and the intensity of each Rho band was quantified by using NIH IMAGE gel plotting macro. Results were expressed as autoradiogram intensity per SDS/PAGE gel intensity, and data were corrected for basal phosphorylation in the absence of α-toxin permeabilization.

Calculation of $[Ca^{2+}]_{free}$. $[Ca^{2+}]_{free}$ was calculated by using the computer program CHELATOR 1.0 (21). Residual Ca^{2+} was removed by passing water through Chelex 100 resin (Sigma). Other procedures related to $[Ca^{2+}]_{free}$ control and measurements have been described (22).

Antibodies. mAb C7 against Rho was generated according to standard procedures (23) by immunizing mice with a 3-[(3-cholamidopropyl)dimethylammonio]-1-propanesulfonate (CHAPS) extract of ROS. The antibody recognized the N-terminal fragment of Rho. Rabbit anti-α-toxin pAb (UW60) was raised in New Zealand White rabbits by subcutaneous immunization with ≈50 μg of bacteria-expressed α-toxin. For Western blots, mAbs anti-GCAP1, G2 (24), anti-RK, G8 (25), anti-arrestin, S65–34 (a gift from G. Adamus, Neurological Sciences Institute, Portland, OR), anti-Rho, 4D2 (a gift from R. S. Molday, University of British Columbia, Vancouver, BC, Canada), and polyclonal antibody against recoverin (a gift from A. S. Polans, University of Wisconsin, Madison, WI) were diluted 1:5,000 or 1:10,000.

Confocal Immunofluorescence Localization of α-Toxin and Neurobiotin on Sections of Bovine Retina. Retinal punches collected from freshly enucleated bovine eyes were transferred to isoosmotic buffer [10 mM Hepes (pH 7.5)/120 mM NaCl/3.5 mM KCl/10 mM glucose/0.2 mM $CaCl_2$/0.2 mM $MgCl_2$/1

mM EDTA] at room temperature. Purified α-toxin (H5K8A) was added to selected samples (50 μg/ml final concentration) and gently mixed. After 20 min, $ZnSO_4$ (4 mM final concentration) was added to selected samples. Following a 10-min incubation, the intracellular tracer *N*-(2-aminoethyl) biotinamide hydrochloride (Neurobiotin, Vector Labs) was added to all samples (4 mM final concentration). Samples were incubated in solution containing Neurobiotin for 30 min. $ZnSO_4$ was added to all samples (4 mM final concentration), which were then rinsed for 20 min twice with gentle agitation in isoosmotic buffer containing 4 mM Zn^{2+}. Retinal punches were rinsed in 140 mM phosphate buffer (pH 7.2) and fixed in 4% paraformaldehyde in phosphate buffer overnight at 4°C. To prepare tissue for confocal immunofluorescence, punches were rinsed for 15 min three times in 140 mM phosphate buffer, embedded in 5% agarose, and sectioned into 100-μm slices on a VT1000E vibrating microtome (Leica). Sections were incubated briefly in immunocytochemistry (ICC) buffer containing PBS (pH 7.2), 0.5% BSA, 0.2% Triton X-100, and 0.05% sodium azide. Normal goat serum (5%) was added to reduce nonspecific immunolabeling. Sections were incubated overnight at 4°C in ICC buffer containing the affinity-purified rabbit polyclonal antibody to α-toxin (UW60, 1:250). After repeated washing in ICC buffer, Cy2-conjugated goat anti-rabbit antibody (Jackson ImmunoResearch) and Cy3-conjugated streptavidin (Jackson ImmunoResearch) were added to sections of retina and incubated overnight at 4°C. Sections were washed thoroughly in ICC buffer, mounted in 5% *n*-propyl gallate in glycerol, and covered with coverslips. Sections were examined on a Bio-Rad 600 laser scanning confocal microscope configured for dual-channel labeling. Gain and black level scan head controls were standardized before images were collected. Raw, unprocessed digital images were converted to PICT format by using Adobe PHOTOSHOP 3.0.

RESULTS

Permeabilization of ROS by α-Toxin. Trephine punches were permeabilized with α-toxin, incubated with [γ-^{32}P]ATP, and exposed to a single flash that bleached ≈10% of Rho. After 5 min, protein kinase and phosphatase inhibitors were added to the samples, which were then immediately frozen on dry ice/ethanol to stop the reaction. ROS disc membranes were partially purified. SDS/PAGE and autoradiography analysis revealed predicted protein (Fig. 2*A*) and phosphorylation (Fig. 2*B*) patterns. High Rho* phosphorylation was detected only in the α-toxin-treated samples. The phosphorylation was light-dependent, in agreement with many studies published previously (reviewed in ref. 1). Under these conditions, chelation of Ca^{2+} does not appear to effect Rho* phosphorylation (Fig. 2*B*). In solubilized trephine punches, the composition of soluble (arrestin) and membrane-associated (GCAP1, RK, and the splice-variant form of arrestin, p^{44}) proteins were comparable for all experimental conditions (Fig. 2*C*). Although the ultrastructure of ROS is maintained in these preparations, the absence of the retinal pigment epithelium prevents the regeneration of Rho. Because arrestin is present at high concentration, it is predicted that dephosphorylation is almost completely inhibited (26). Therefore, we were able to analyze Rho* phosphorylation without interference associated with concurrent dephosphorylation.

Application of Zn^{2+}-Gated α-Toxin. The Zn^{2+}-switchable pore offers several advantages over the wild-type pore. Most importantly, low molecular weight marker molecules (fluorescent tracers, for example) that have been introduced into the cell can be retained during reactions or during washing procedures. Immunofluorescent labeling and confocal microscopy were used to demonstrate the subcellular distribution and permeability of Zn^{2+}-sensitive (H5K8A) α-toxin pores formed in bovine photoreceptors. Photoreceptors incubated in buffer

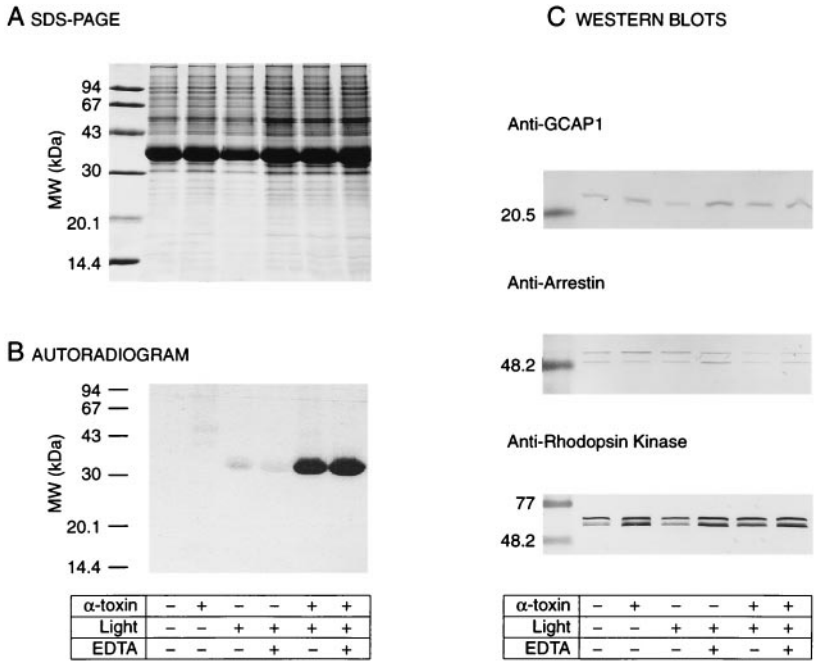

FIG. 2. Assay for Rho* phosphorylation in α-toxin-permeabilized retina. (*A*) SDS/PAGE. Retina punches (7.5 mm in diameter) were incubated under various experimental conditions. ROS were then purified, solubilized in 1% SDS, and a fraction (10 μl) of each sample was subjected to SDS/PAGE on a 12% gel. The amounts of Rho were comparable in all conditions. (*B*) Autoradiogram of the SDS/PAGE gel. Samples kept in the dark showed no phosphorylation in the presence or absence of α-toxin (lanes 1 and 2). In samples exposed to light, an increase in radiolabeled phosphorylation of Rho* in retina permeabilized with α-toxin (100 μg/ml) is clearly visible (lanes 5 and 6) as compared with nonpermeabilized retina (lanes 3 and 4). EDTA (4 mM) was added to the incubation buffer (lanes 4 and 6) as a control for nonspecific phosphorylation or phosphorylation resulting from broken ROS. (*C*) Western blots. ROS samples were immunoblotted and labeled with antibodies against several ROS proteins (GCAP1, arrestin, and rhodopsin kinase). α-Toxin is required for the light-dependent phosphorylation, and permeabilized retina retains protein >20 kDa.

containing α-toxin (Fig. 3 *A* and *B*) were immunolabeled with an affinity-purified antibody for this pore-forming protein. α-Toxin immunolabeling (green) is heaviest in the plasma membrane surrounding outer segments (OS), with lighter labeling of the plasma membrane surrounding the rod inner segments (IS). No immunolabeling was observed in photoreceptors incubated in buffer from which the α-toxin was omitted (Fig. 3 *C* and *D*). Neurobiotin, a low molecular weight compound used widely in intracellular labeling studies, was employed to evaluate the permeability of α-toxin pores in the presence or absence of Zn^{2+} ions. Neurobiotin (red; labeled with streptavidin Cy3) is abundant throughout the cytoplasm of photoreceptor OSs and ISs that contain the pore in an open, Zn^{2+}-free state (Fig. 3*A*). Pretreatment of α-toxin-permeabilized photoreceptors with Zn^{2+}-containing buffer (4 mM) triggers the closure of these pores, thereby excluding Neurobiotin from the photoreceptor cytoplasm (Fig. 3*B*). Exclusion of neurobiotin from photoreceptors without α-toxin treatment (Fig. 3 *C* and *D*) or retinas containing the α-toxin pore in a closed state (Fig. 3*B*) confirm that the permeability of this pore can be manipulated easily and that the treatment and incubation conditions alone do not adversely affect the integrity of the plasma membrane surrounding these cells.

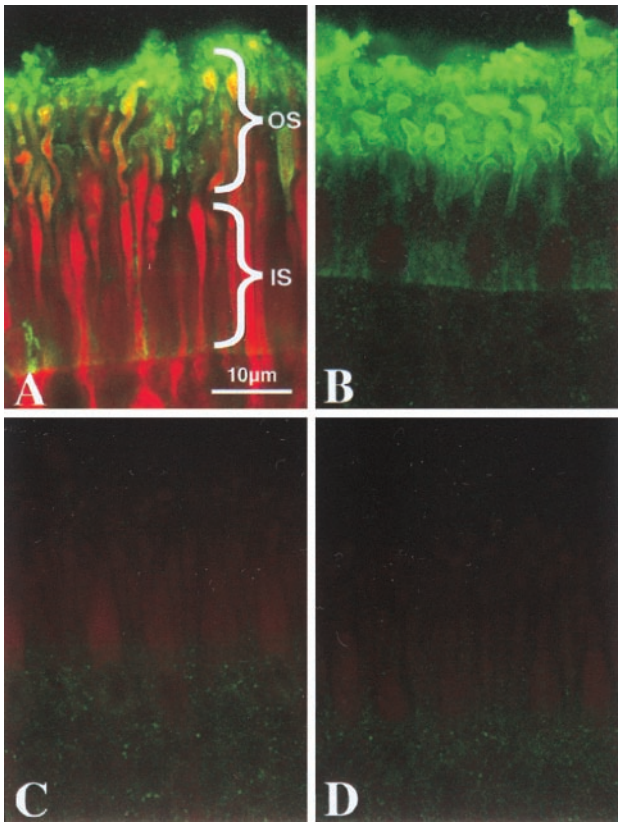

FIG. 3. Permeability of rod plasma membranes containing the Zn^{2+}-sensitive form of the α-toxin pore (H5K8A) demonstrated by confocal fluorescence localization of low molecular weight intracellular tracer. Retinal punches were incubated in the presence (*A* and *B*) or absence (*C* and *D*) of α-toxin. The addition of Zn^{2+} to the incubation medium causes pore closure (*B* and *D*). The low molecular weight intracellular tracer *N*-(2-aminoethyl) biotinamide hydrochloride (Neurobiotin) was added to all samples to assess permeability of α-toxin pores under various conditions. An α-toxin-specific polyclonal antibody was used to immunolocalize this protein (green). α-Toxin is restricted to the plasma membrane-surrounding rod inner segments (IS) and outer segments (OS) of treated retinas (*A* and *B*). Streptavidin-Cy3 was used to localize neurobiotin in these samples (red). Neurobiotin is present in the cytoplasm of rod OS and IS (*A*), confirming that α-toxin forms functional pores in these cells. Neurobiotin is prevented from diffusing through α-toxin pores closed by Zn^{2+} (*B*).

Rho* phosphorylation was observed in α-toxin-treated retina punches in the presence and absence of Zn^{2+} each time the cells were loaded with [γ-^{32}P]ATP (Fig. 4). Rho* phosphorylation was undetectable, however, when the Zn^{2+}-sensitive mutant α-toxin was used and the pore was closed with 4 mM $ZnSO_4$ before addition of [γ-^{32}P]ATP (Fig. 4). In control experiments with native α-toxin, the addition of Zn^{2+} did not affect Rho* phosphorylation. In these experiments, and in all experiments described below, Rho was rapidly isolated by affinity chromatography in the presence of protein kinase and phosphatase inhibitors to prevent dephosphorylation. A similar mobility of Rho and peripherin in SDS/PAGE analysis and the possibility of contamination by cone pigments and peripherin/rds, which was reported to be phosphorylated (27), was our main concern. Cone pigments and peripherin/rds did not interfere, however, with the phosphorylation analysis (Fig. 5*A*), because the results did not differ significantly between the two methods of Rho isolation.

Phosphorylation of Rho* at Different $[Ca^{2+}]_{free}$ Levels. The Rho* phosphorylation reactions were set up under two different conditions of $[Ca^{2+}]_{free}$, reproducing the physiological concentrations. Rho was isolated (Fig. 5*A*, *a*) and identified by Western blot analysis (Fig. 5*A*, *b*). Phosphorylation of Rho*

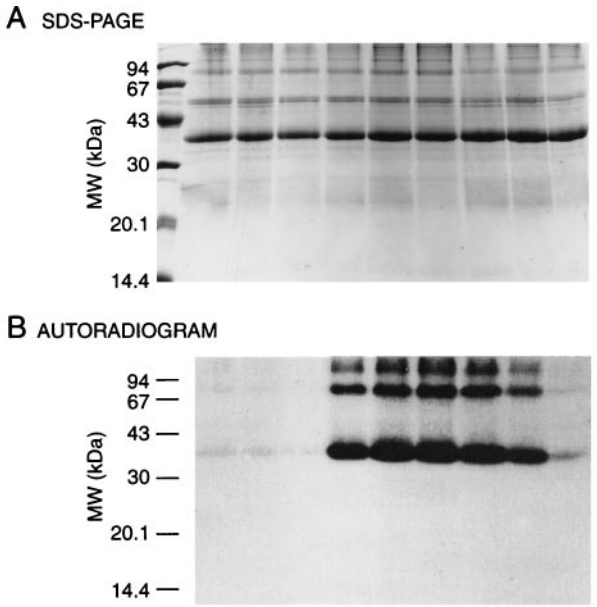

α-toxin	None			K8A			H5K8A		
Zn^{2+} added before ATP	−	−	+	−	−	+	−	−	+
Zn^{2+} added after ATP	−	+	−	−	+	−	−	+	−

FIG. 4. The effect of Zn^{2+} on Rho* phosphorylation in retina permeabilized by the Zn^{2+}-sensitive α-toxin mutant. "Pseudo" wild-type (K8A) α-toxin and a mutated form (H5K8A), closable by Zn^{2+}, were used to permeabilize retinas. (*A*) After retinal punches were incubated under various experimental conditions, Rho was purified by immunoaffinity, quantified by the Bradford method (42), and the same amounts of protein were subjected to a 12% SDS/PAGE. (*B*) Autoradiogram of phosphorylated Rho*. Radioactive phosphorylation is only visible in samples permeabilized with α-toxin [lanes 4–8 compared with lanes 1–3 (no α-toxin)]. When Zn^{2+} was added before [γ-^{32}P]ATP, the nucleotide entered the cell though the WT(K8A) α-toxin pore, and phosphorylation was detected (lane 6). On the contrary, little phosphorylation was observed when the mutated α-toxin (H5K8A) was used (lane 9), i.e., the pore was closed before [γ-^{32}P]ATP could get in the cells. When Zn^{2+} was added after [γ-^{32}P]ATP, radioactive phosphorylation was observed for both forms of toxin (lanes 5 and 8).

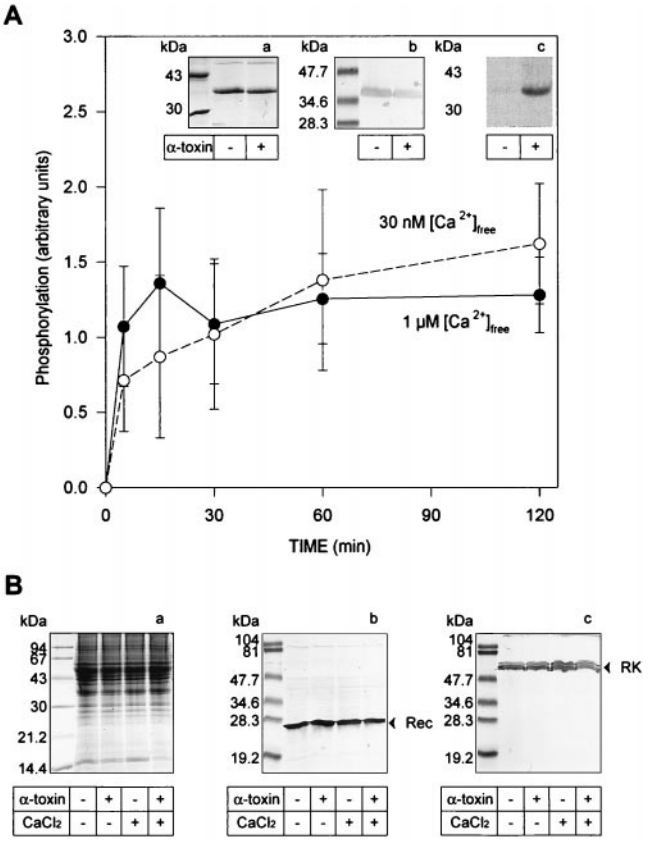

FIG. 5. Phosphorylation rate is not affected by Ca^{2+} concentration. (*A*) Kinetics of Rho* phosphorylation were analyzed at 30 nM (○) and 1 μM (●) $[Ca^{2+}]_{free}$. Both experiments were done in parallel; only the $[Ca^{2+}]_{free}$ in the incubation buffer was different. After incubation of retina punches with α-toxin and the addition of [γ-^{32}P]ATP in the dark, the phosphorylation reaction was started at $t = 0$ by a flash. At the end of the reaction (*Inset*), punches were solubilized and Rho was affinity-purified. (*a*) Coomassie staining, (*b*) Western blot probed with a second anti-Rho mAb, and (*c*) autoradiogram. Only the retina treated with α-toxin showed Rho radioactive phosphorylation ($t = 60$ min). (*B*) Western blot analysis of trephine punches. Before Rho purification, solubilized punches incubated with or without α-toxin and at low or high $[Ca^{2+}]_{free}$ were analyzed for recoverin or RK content. (*a*) Coomassie staining, (*b*) Western blots probed with a polyclonal antibody against recoverin, and (*c*) Western blots probed with a mAb against RK.

was detected only when rods were permeabilized with α-toxin (Fig. 5*A*, *c*) and appears to be unaffected by $[Ca^{2+}]_{free}$ ($n = 12$). As before, the amounts of recoverin and RK in our assays were comparable in all experimental conditions (Fig. 5*B*).

Closure of the pore after the ROS are loaded with [γ-^{32}P]ATP may allow reestablishment of intracellular conditions similar to the native conditions. To allow the permeabilized cells to achieve their cationic balance, the pore was closed with Zn^{2+} and phosphorylation was tested in the presence of different concentrations of external $[Ca^{2+}]_{free}$. As shown in Fig. 6 ($n = 7$), the Rho* phosphorylation plateau (at ≈5 min) was not affected by the presence of different $[Ca^{2+}]_{free}$. The estimated phosphorylation stoichiometry was ≈0.3–0.5 phosphate per Rho*, in agreement with studies on Rho phosphorylation *in vivo* using a mouse model (13). Not all Rho* molecules are phosphorylated, and the reason for this observation is unknown.

DISCUSSION

α-Toxin-Treated Bovine Retina as a Model for Studying Phototransduction. The α-toxin-treated bovine retina provides a unique experimental approach for studying phototransduction. Introduction of small metabolites into the minimally compromised ROS may allow monitoring of any step of phototransduction for which radioactive tracers or other analytical tools are available. Such studies minimize artifacts associated with the use of cell homogenates. Additional advantages of the system include the ability to control the ionic status within photoreceptors at physiologically correct stoichiometries and concentrations of proteins. A decrease in $[Ca^{2+}]_{free}$ during phototransduction is the principal mechanism involved in controlling the sensitivity of photoreceptors (28, 29). In addition to Ca^{2+} ions, this regulation involves Ca^{2+}-binding proteins. Recoverin, one of the retinal Ca^{2+}-binding proteins, was implicated in regulation of Rho* phosphorylation by direct binding to RK and inhibition of its activity (see below). This type of regulation was proposed for calmodulin and other G protein-coupled receptor kinases in cells where $[Ca^{2+}]_{free}$ is elevated as a result of cell stimulation (30).

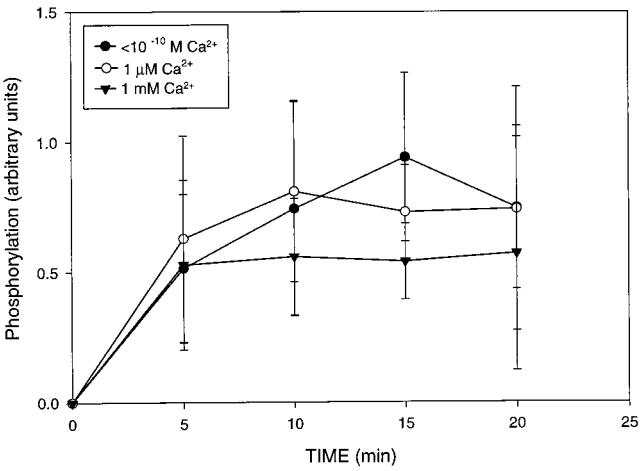

FIG. 6. Effect of extracellular variation of $[Ca^{2+}]_{free}$ on Rho* phosphorylation in retina with closed α-toxin pores. After incubation of punches of retina with α-toxin in the presence of 1 μM $[Ca^{2+}]_{free}$ and addition of [γ-^{32}P]ATP in the dark, pores were closed by the addition of $ZnSO_4$ and punches were transferred to a new incubation buffer containing variable $[Ca^{2+}]_{free}$ (1 μM, 1 mM, or 10^{-10} M). The phosphorylation reactions were started at $t = 0$ by a flash.

Does Recoverin Modulate RK Activity? There are a few inconsistencies with the proposed mechanism of RK regulation by recoverin under physiological conditions. First, at high $[Ca^{2+}]_{free}$ in the dark, according to the model of RK regulation by recoverin, RK is in an inactive complex with recoverin (6–9). Activation of Rho results in a rapid decrease in cGMP. Because cGMP is gating the Ca^{2+} influx through the channel, compensated by continuous efflux through Na^+/Ca^{2+}–K^+ exchanger, a decrease in cGMP is closely followed by a decrease in Ca^{2+}. During this initial phase, when $[Ca^{2+}]_{free}$ is still high, RK could be modulated by recoverin, regulating the gain of transducin activation. The initial decrease in the circulating current, however, is not under control of phosphorylation, because the amplification phase of phototransduction is unaffected by the presence or absence of ATP (31) or the addition of extra RK or arrestin to ROS homogenates (32); neither is the amplification phase affected in transgenic mice lacking the C terminus of Rho (33) or arrestin (34). In all of these studies, the kinetics of the initial phase of phototransduction remain similar; only the final amplitude varies. Until the circulating dark current recovers, the rest of the phototransduction cascade will experience low $[Ca^{2+}]_{free}$. In these conditions, recoverin is in a Ca^{2+}-free form and does not interact with RK. Second, the decrease in the dark current is closely followed by the decrease in $[Ca^{2+}]_{free}$; however, if the

recovery of the circulating current occurs rapidly, restoration of the $[Ca^{2+}]_{free}$ is delayed, likely by the buffering ability of ROS (35). This suggests that even in the latest phase of phototransduction, the recoverin regulation of Rho* phosphorylation would have to occur at a low $[Ca^{2+}]_{free}$, where recoverin is inactive. In fact, the low affinity of recoverin (K_d = 2–13 μM; refs. 8 and 36) for Ca^{2+} (for comparison, the affinity of GCAP1 for Ca^{2+} is 10–40 times higher , K_d = 0.3 μM, ref. 24) almost excludes a role for recoverin in the recovery phase. Third, the regulation of RK activity by recoverin was proposed to be involved in light adaptation (12). However, Ohguro *et al.* (2) showed that background illumination, i.e., a lower $[Ca^{2+}]_{free}$ and potentially more RK available, doesn't increase the level of phosphorylation of Rho* in response to a single flash. On the contrary, these authors reported a decrease in Rho* phosphorylation triggered by a flash in samples that were light adapted. Fourth, from a recent study of a patient suffering from Oguchi disease, a recessively inherited retinopathy caused by the deletion of exon 5 of RK (5), it appears that RK may have only a minor role in light adaptation. In the homozygous subject, adaptation was normal at low backgrounds and only became abnormal at higher backgrounds. Fifth, the functional range of illumination of a rod produces on the order of 10,000 isomerizations of Rho molecules per sec. ROS have 10^8 Rho molecules (3 mM) and about 10^5–10^6 molecules (3–30 μM) of RK and recoverin. A weak interaction between RK and Ca^{2+}-recoverin (K_d = 1–5 μM; refs. 7, 8, 37) will leave 1/3 to 2/3 of the RK molecules dissociated from Ca^{2+}-recoverin, even if one does not consider that the majority of RK will be autophosphorylated and unable to interact with recoverin (10). Furthermore, a competition between Rho* and recoverin for RK binding will result in only a partial inhibition of RK. Because a heterozygote for the null RK mutation appears to have normal functional rods and a robust inactivation mechanism (5), i.e., only half of the normal RK is needed to efficiently inactivate Rho*, a partial inhibition of RK is insufficient to account for a major role in the kinetics of inactivation. In contrast, it is worth noting that the affinity between calmodulin and other GRKs are in the range of 10–50 nM (30). Finally, whereas virtually all phototransduction proteins are expressed exclusively in photoreceptors and localize preferentially to the OS, recoverin displays a more diverse pattern of expression that includes not only photoreceptors but also cone bipolar cells (38).

In this study, we find no evidence of Ca^{2+} regulation of Rho* phosphorylation in our preparations under a broad range of experimental conditions. This observation is in contrast to recent studies that used biochemical reconstitution assays. This difference may be a result of immense dilutions of those reconstitution assays and the lack of a putative functional target for recoverin. These problems were avoided by using α-toxin-permeabilized photoreceptors. The role of recoverin in phototransduction remains unanswered. This evolutionarily conserved retinal protein, expressed to high levels in photoreceptor cells and a subset of bipolar cells, clearly inhibits the rate of recovery of dark current in electrophysiological experiments (36, 39–41). The apparent interactions *in vitro* between recoverin and RK may be magnified by the loss of other ROS proteins or by the addition of a large excess of exogenous recoverin. Under physiological conditions, however, recoverin may simply play a role as a Ca^{2+} buffer.

We thank Dr. H. Bayley for the clones of α-toxins, Dr. J. C. Saari for critical comments on the manuscript, and Grace P. Yang for outstanding help during the course of these studies. Confocal studies were conducted through the Keck Center for Advanced Studies in Neural Signaling at the University of Washington with the assistance of P. Brunner. This research was supported by Grant EY08061 from the National Institutes of Health and an award from Research to Prevent Blindness, Inc. to the Department of Ophthalmology at the University of Washington. K.P. is a recipient of a Jules and Doris Stein Professorship from Research to Prevent Blindness.

1. Palczewski, K. (1997) *Eur. J. Biochem.* **248,** 261–269.
2. Ohguro, H., Rudnicka-Nawrot, M., Buczylko, J., Zhao, X., Taylor, J. A., Walsh, K. A. & Palczewski, K. (1996) *J. Biol. Chem.* **271,** 5215–5224.
3. Palczewski, K., Buczylko, J., Kaplan, M. W., Polans, A. S. & Crabb, J. W. (1991) *J. Biol. Chem.* **266,** 12949–12955.
4. Yamamoto, S., Sippel, K. C., Berson, E. L. & Dryja, T. P. (1997) *Nat. Genet.* **15,** 175–178.
5. Cideciyan, A. V., Zhao, X., Nielsen, L., Khani, S. C., Jacobson, S. G. & Palczewski, K. (1998) *Proc. Natl. Acad. Sci. USA* **95,** 328–333.
6. Kawamura, S. (1993) *Nature (London)* **362,** 855–857.
7. Chen, C. K., Inglese, J., Lefkowitz, R. J. & Hurley, J. B. (1995) *J. Biol. Chem.* **270,** 18060–18066.
8. Klenchin, V. A., Calvert, P. D. & Bownds, M. D. (1995) *J. Biol. Chem.* **270,** 16147–16152.
9. Sato, N. & Kawamura, S. (1997) *J. Biochem.* **122,** 1139–1145.
10. Satpaev, D. K., Chen, C. K., Scotti, A., Simon, M. I., Hurley, J. B. & Slepak, V. Z. (1998) *Biochemistry* **37,** 10256–10262.
11. Matsuda, S., Hisatomi, O., Ishino, T., Kobayashi, Y. & Tokunagati, F. (1998) *J. Biol. Chem.* **273,** 20223–20227.
12. Kawamura, S. (1994) *Neurosci. Res. (N.Y.)* **20,** 293–298.
13. Ohguro, H., Van Hooser, J. P., Milam, A. H. & Palczewski, K. (1995) *J. Biol. Chem.* **270,** 14259–14262.
14. Bhakdi, S., Bayley, H., Valeva, A., Walev, I., Walker, B., Kehoe, M. & Palmer, M. (1996) *Arch. Microbiol.* **165,** 73–79.
15. Bhakdi, S. & Tranum-Jensen, J. (1991) *Microbiol. Rev.* **55,** 733–751.
16. Binder, B. M., Biernbaum, M. S. & Bownds, M. D. (1990) *J. Biol. Chem.* **265,** 15333–15340.
17. Song, L., Hobaugh, M. R., Shustak, C., Cheley, S., Bayley, H. & Gouaux, J. E. (1996) *Science* **274,** 1859–1866.
18. Walker, B., Kasianowicz, J., Krishnasastry, M. & Bayley, H. (1994) *Protein Eng.* **7,** 655–662.
19. Walker, B. & Bayley, H. (1994) *Protein Eng.* **7,** 91–97.
20. Walker, B., Krishnasastry, M., Zorn, L., Kasianowicz, J. & Bayley, H. (1992) *J. Biol. Chem.* **267,** 10902–10909.
21. Schoenmakers, T. J., Visser, G. J., Flik, G. & Theuvenet, A. (1992) *BioTechniques* **12,** 870–874, 876–879.
22. Rudnicka-Nawrot, M., Surgucheva, I., Hulmes, J. D., Haeseleer, F., Sokal, I., Crabb, J. W., Baehr, W. & Palczewski, K. (1998) *Biochemistry* **37,** 248–257.
23. Campbell, A. M. (1984) *Monoclonal Antibody Technology* (Elsevier, Amsterdam).
24. Gorczyca, W. A., Polans, A. S., Surgucheva, I. G., Subbaraya, I., Baehr, W. & Palczewski, K. (1995) *J. Biol. Chem.* **270,** 22029–22036.
25. Zhao, X., Huang, J., Khani, S. C. & Palczewski, K. (1998) *J. Biol. Chem.* **273,** 5124–5131.
26. Palczewski, K., McDowell, J. H., Jakes, S., Ingebritsen, T. S. & Hargrave, P. A. (1989) *J. Biol. Chem.* **264,** 15770–15773.
27. Boesze-Battaglia, K., Kong, F., Lamba, O. P., Stefano, F. P. & Williams, D. S. (1997) *Biochemistry* **36,** 6835–6846.
28. Koutalos, Y. & Yau, K. W. (1996) *Trends Neurosci.* **19,** 73–81.
29. Polans, A., Baehr, W. & Palczewski, K. (1996) *Trends Neurosci.* **19,** 547–554.
30. Chuang, T. T., Paolucci, L. & De Blasi, A. (1996) *J. Biol. Chem.* **271,** 28691–28696.
31. Gray-Keller, M. P., Detwiler, P. B., Benovic, J. L. & Gurevich, V. V. (1997) *Biochemistry* **36,** 7058–7063.
32. Langlois, G., Chen, C. K., Palczewski, K., Hurley, J. B. & Vuong, T. M. (1996) *Proc. Natl. Acad. Sci. USA* **93,** 4677–4682.
33. Chen, J., Makino, C. L., Peachey, N. S., Baylor, D. A. & Simon, M. I. (1995) *Science* **267,** 374–377.
34. Xu, J., Dodd, R. L., Makino, C. L., Simon, M. I., Baylor, D. A. & Chen, J. (1997) *Nature (London)* **389,** 505–509.
35. Gray-Keller, M. P. & Detwiler, P. B. (1994) *Neuron* **13,** 849–861.
36. Erickson, M. A., Lagnado, L., Zozulya, S., Neubert, T. A., Stryer, L. & Baylor, D. A. (1998) *Proc. Natl. Acad. Sci. USA* **95,** 6474–6479.
37. Senin, I. I., Dean, K. R., Zargarov, A. A., Akhtar, M. & Philippov, P. P. (1997) *Biochem. J.* **321,** 551–555.
38. Milam, A. H., Dacey, D. M. & Dizhoor, A. M. (1993) *Visual Neurosci.* **10,** 1–12.
39. Kawamura, S. & Murakami, M. (1991) *Nature (London)* **349,** 420–423.
40. Gray-Keller, M. P., Polans, A. S., Palczewski, K. & Detwiler, P. B. (1993) *Neuron* **10,** 523–531.
41. Baylor, D. (1996) *Proc. Natl. Acad. Sci. USA* **93,** 560–565.
42. Bradford, M. M. (1976) *Anal. Biochem.* **72,** 248–254.